Redox Biology 70 (2024) 103006

Contents lists available at ScienceDirect

Redox Biology

journal homepage: www.elsevier.com/locate/redox

Therapeutic effects of long-term HBOT on Alzheimer's disease neuropathologies and cognitive impairment in *APP^{swe}/PS1^{dE9}* mice

Cui Yang [a], Guangdong Liu [a], Xianrong Zeng [b], Yang Xiang [a], Xi Chen [a], Weidong Le [a,*]

[a] Institute of Neurology, Sichuan Provincial People's Hospital, School of Medicine, University of Electronic Science and Technology of China, Chengdu, 610054, China
[b] Department of Hyperbaric Oxygen, Sichuan Provincial People's Hospital, University of Electronic Science and Technology of China, Chengdu, China

ARTICLE INFO

Keywords:
Alzheimer's disease
Long-term hyperbaric oxygen therapy
Amyloid plaques deposition
Blood oxygen saturation
Neuroinflammatory

ABSTRACT

Alzheimer's disease (AD) is the most common neurodegenerative disorder with the pathological hallmarks of amyloid beta (Aβ) plaques and neurofibrillary tangles (NFTs) in the brain. Although there is a hope that anti-amyloid monoclonal antibodies may emerge as a new therapy for AD, the high cost and side effect is a big concern. Non-drug therapy is attracting more attention and may provide a better resolution for the treatment of AD. Given the fact that hypoxia contributes to the pathogenesis of AD, hyperbaric oxygen therapy (HBOT) may be an effective intervention that can alleviate hypoxia and improve AD. However, it remains unclear whether long-term HBOT intervention in the early stage of AD can slow AD progression and ultimately prevent cognitive impairment in this disease. In this study we applied consecutive 3-month HBOT interventions on 3-month-old *APP^{swe}/PS1^{dE9}* AD mice which represent the early stage of AD. When the *APP^{swe}/PS1^{dE9}* mice at 9-month-old which represent the disease stage we measured cognitive function, 24-h blood oxygen saturation, Aβ and tau pathologies, vascular structure and function, and neuroinflammation in *APP^{swe}/PS1^{dE9}* mice. Our results showed that long-term HBOT can attenuate the impairments in cognitive function observed in 9-month-old *APP^{swe}/PS1^{dE9}* mice. Most importantly, HBOT effectively reduced the progression of Aβ plaques deposition, hyperphosphorylated tau protein aggregation, and neuronal and synaptic degeneration in the AD mice. Further, long-term HBOT was able to enhance blood oxygen saturation level. Besides, long-term HBOT can improve vascular structure and function, and reduce neuroinflammation in AD mice. This study is the first to demonstrate that long-term HBOT intervention in the early stage of AD can attenuate cognitive impairment and AD-like pathologies. Overall, these findings highlight the potential of long-term HBOT as a disease-modifying approach for AD treatment.

1. Introduction

Alzheimer's disease (AD) is an insidious neurodegenerative condition that manifests itself as a progressive decline in memory and cognitive function, disable to perform daily living activities, and is usually accompanied by various mental symptoms and behavioral disorders [1]. AD is pathologically characterized by progressive neuronal and synaptic loss in the brain, resulting from the deposition of amyloid-beta (Aβ) plaques and phosphorylated tau neurofibrillary tangles [2,3]. The treatment of AD involves in general the combination of different therapeutic approaches such as pharmacological and non-pharmacological interventions [4,5]. Monoclonal antibodies against Aβ aggregation are a new approach for the AD treatment [4]; other non-drug therapies such as light treatment [6], music therapy [7], and exercise [8] are attracting more attention.

Hypoxia usually results from environmental and pathological factors including aging, cerebrovascular diseases, hypertension, type 2 diabetes, traumatic brain injury, and sleep disordered breathing [9]. Hypoxia is closely linked to the pathogenesis of AD [10,11], which can lead to abnormal Aβ metabolism and tau phosphorylation, as well as neuronal and synaptic degeneration. Since hypoxia contributes to the development of AD, the anti-hypoxia therapy may be a potential therapeutic strategy to improve the clinical manifestations and pathological biochemical processes of the disease [12].

Hyperbaric oxygen therapy (HBOT) is an intervention that involves administering 100 % oxygen at a pressure greater than 1 atm absolute (ATA) [13]. HBOT can effectively increase the amount of oxygen dissolved in plasma and the partial pressure of arterial oxygen, thereby

* Corresponding author.
E-mail address: wdle@sibs.ac.cn (W. Le).

https://doi.org/10.1016/j.redox.2023.103006
Received 23 October 2023; Received in revised form 1 December 2023; Accepted 18 December 2023
Available online 23 December 2023

correcting or alleviating hypoxia [14]. And there is evidence of positive effects of HBOT on neurological outcomes after cerebral ischemia [15] and moderate traumatic brain injury [16]. Studies conducted by our group and others have suggested that HBOT significantly enhances cognitive function in patients or animal models of AD [12]. However, existing studies have only provided preliminary insights into the short-term effectiveness and potential mechanisms of short-term HBOT in the middle and late stages of AD. But it is unclear whether long-term HBOT intervention in early AD can slow the disease progression and ultimately prevent cognitive impairment. Therefore, it is of importance to investigate the safety, long-term efficacy and possible mechanisms of long-term HBOT treatment for AD [17].

In AD, the cerebrovascular system undergoes significant morphological and structural changes that alter the regulation of blood flow, vascular fluid dynamics, and vascular integrity, leading to reduced cerebral blood flow and vascular dysfunction [18]. However, decreased cerebral blood flow (CBF) [19] and vascular dysfunction may limit Aβ clearance, further aggravate hypoxia and oxidative stress [20]. HBOT has the potential to regulate the structure and morphology of blood vessels [21] and increase CBF [22]. Therefore, HBOT may have the potential to attenuate AD by improving cerebral blood flow and vascular dysfunction. In addition, neuroinflammation, characterized by activation of the brain's innate immune system, plays a crucial role in the pathophysiology of AD [23]. It has been reported that hypoxia can aggravate neuroinflammation and lead to increased nerve damage [10,11]. It is proposed that HBOT may reduce the neuroinflammatory process by alleviating the activation of astrocytes and microglia [24,25].

In this study, we examined the effects of long-term HBOT on AD-related cognitive function and neuropathology, and explored the underlying mechanisms against AD. The findings from this study may provide new insights into the HBOT therapy for clinical use in AD.

2. Materials and methods

2.1. Experimental animals

Male $APP^{swe}/PS1^{dE9}$ transgenic mice and their age-matched wild-type (WT) littermates in this study were purchased from the Jackson Laboratory (Bar Harbor, MA, USA). All the mice were housed under the condition of controlled light (12 h/12 h light/dark cycle), constant room temperature 22 ± 1 °C and relative humidity 50 ± 10 %. All animal experiments were conducted in accordance with the guidelines approved by the Committee on the Ethics of Animal Experiments and the Institutional Animal Care and Use Committee at Sichuan Provincial People's Hospital.

The mice at the age of 3 months were randomized into four groups: AD with HBOT(AD-H), AD with normoxia (AD-N), WT with HBOT (WT-H), WT with normoxia (WT-N). The AD-H and WT-H mice were subjected to HBOT for 3 months, and the mice were evaluated for learning and memory after 3 months of HBOT, and then sacrificed for neuropathological and biochemical examinations.

2.2. Hyperbaric oxygen therapy

For the HBOT, animals were administered 100 % oxygen at a pressure of 2 ATA in a custom-made mono-chamber intended for small animals for 60 min daily for 90 consecutive days. Before compression was initiated, the mono-chamber was washed with 100 % oxygen for 5 min to enrich oxygen content. Compression and decompression were performed gradually within 25 min. Oxygen level inside the chamber following compression reached saturation of ≥96 %, as measured by an oxygen analyzer. The animals in the control, non-treated group, were placed inside the mono-chamber for 60 min without additional treatment (at 1 ATA). Temperature, measured with a temperature controller during all sessions for HBOT and control groups in the mono-chamber, was similar among the four groups.

2.3. Measurement of blood oxygen saturation

Pulse oximeters (STARR Life Sciences® Corp) were used to monitor the oxygen saturation of experimental mice in real-time while awake [26]. The day before the experiment, we shaved the necks of all mice because dark hairs interfere with detecting light signals. At the same time, we clamped the test clips on the necks of the mice and placed them in the experimental cage to adapt to the environment. When the experiment began, we turned on the pulse oximeter, selected the awake mode, and set the parameters. The sensor was clipped to the neck of the experimental mouse (where the carotid artery pulsates) and the changes in blood oxygen saturation in the mice were monitored for 24 h. We averaged the data every 10 min. Oxygen saturation fluctuations were expressed by the coefficient of variation (CV) (standard deviation/mean*100) [27].

2.4. Routine blood test

Peripheral blood was taken from the epicanthal veins of mice. After taking the blood, the capillary glass tube was removed, and the mouse's skin was pressed with a cotton ball to stop bleeding. Then, 50 μL of blood was placed in the automatic blood cell counter (Beijing Baolingman Sunlight Technology Co.BM830). The system automatically detected various parameters following the manufacturer's instructions.

2.5. Cognitive and motor activity measurements

2.5.1. Morris water maze test

Each mouse was forced to find a submerged escape platform in a circular pool filled with water (25–26 °C) rendered opaque (white) with powdered milk. During the familiarization session and acquisition phase (four trials/day for four consecutive days), the mouse was given as long as 60 s to find the hidden platform and then required to remain seated on this platform for 5 s, after which it was returned to its home cage. During the retention phase, the platform was removed from the pool and for 60s the path taken by each mouse was video-filmed to determine the time required to swim to the original position of the platform as well as the number of passes over and time spent at this position [28].

2.5.2. Shuttle box test

Mice were initially exposed to light and buzzing sound, each lasting 5 s, followed by a 5-s electrical stimulation at a current intensity of 0.7 mA. The mice' responses were categorized as active avoidance if they escaped to the safe zone within 5 s after the onset of the light or sound, or as passive avoidance if they only escaped to the safe zone after the electrical stimulation. Through repeated training sessions (25 in total), the mice gradually developed conditioned responses of active avoidance, leading to the acquisition of memory, followed by the test according to the same procedure as the training phase.

2.5.3. Open field test

The open field test (JLBehv-LAG-6-6, Shanghai Ge-measurement) was performed to evaluate the exploratory behavior and general activity of experimental animals in a novel environment. The open-field test was performed in a square box. A mouse was placed in a corner of the box at the beginning of the test. The number of rearing and total distance traveled in the open field and were measured in a 5-min session.

2.6. Laser speckle contrast imaging

Laser speckle flowmetry obtains high-resolution, two-dimensional imaging and has a linear relationship with absolute CBF values. An anesthesia mask for mice was used for isoflurane inhalation. The skull was placed 10 cm below the scan head and the scalp was removed by a midline incision to expose the skull throughout CBF evaluation. CBF was measured in identically-sized regions of interest (circle 1 mm in

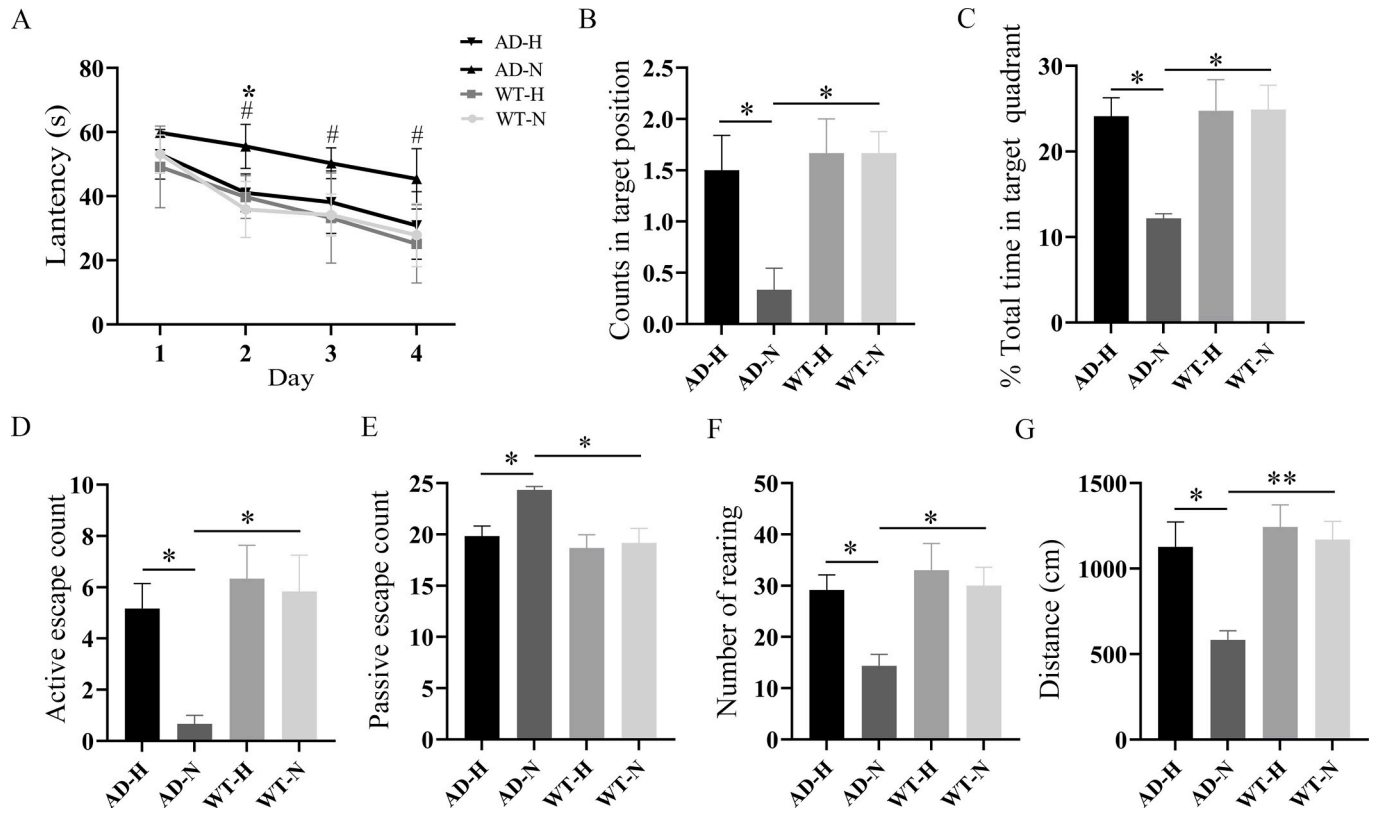

Fig. 1. HBOT improves Cognitive function. (A) The escape latency of mice during the training period after HBOT. (B) The number of times mice passed through the targeted position in quadrant after HBOT. (C) The percentage of swimming time in the target platform quadrant of AD and WT mice in the total swimming time during Morris water maze test period. (D) The active escape count in shuttle box test of mice in each group. (E) The passive escape count in shuttle box test of mice in each group. (F) The number of rearing in open field test of mice in each group. (G) Total distance of mice in open field test. In (A), *represents AD-H vs. AD-N; # represents AD-N vs.WT-N. Data were the mean ± SEM values, with 6 mice per group.*$p < 0.05$, **$p < 0.01$, ***$p < 0.001$, ****$p < 0.0001$, by two-way ANOVA with Tukey's multiple comparisons test.

diameter), located 1 mm posterior and 2 mm lateral from the bregma, corresponding to regions around Heubner's anastomoses, connecting the dorsal branches of the anterior cerebral artery and the middle cerebral artery. Average CBF values in the bilateral hemispheres were recorded [29–31].

2.7. Brain sampling, histology and quantification

After completing the behavioral test, animals were euthanized by overdosing with isopentane. Blood was sampled from the right atrium of the heart, followed by intracardial perfusion with 100 ml of 0.1 % $NaNO_2$ in phosphate buffer. Brains were sampled and weighed. Left hemispheres were fixed in 4 % paraformaldehyde for histological analysis, and right hemispheres were snap frozen in liquid nitrogen and stored at −80 °C for biochemical analysis.

2.7.1. Aβ plaques and tau pathology

For Aβ plaques in parenchyma, brain tissue sections were stained with Congo red for compact Aβ plaques or with 6E10 antibody using a free-floating immunohistochemistry (IHC) method for total Aβ plaques containing compact and diffuse plaques. The primary antibodies are listed in Supplementary Table 1. Immunofluorescence was used to detect phosphorylated tau with *anti*-p-Tau Thr231 antibody. In histology and quantification, a series of five equally spaced tissue sections (~1.3 mm apart) spanning the entire brain of each mouse were used for IHC and immunofluorescence staining. High-magnification images were acquired using biological microscope (Olympus, BX53) or confocal laser scanning microscope (Olympus, FV3000). The area fraction and plaque number of Congo red- or 6E10-positive staining in cortex and hippocampus were quantified with ImageJ. The area fraction of p-Tau Thr231 positive staining in cortex and hippocampus were quantified with ImageJ.

2.7.2. Detections of neurodegeneration, cerebral amyloid angiopathy and neuroinflammation

Neuronal loss and neurite degeneration were detected by double immunofluorescence staining for NeuN and microtubule associated protein (MAP)-2. Immunofluorescence was also used to detect synapsis with SYP. Illustration of cerebral amyloid angiopathy (CAA) by immunofluorescence with the antibody to Aβ (6E10) and smooth muscle in the vessel wall (1A4). Immunofluorescence also be used to visualize microgliosis and astrocytosis with ionized calcium binding adapter molecule 1 (Iba1) antibody to detect activated microglia and anti-glial fibrillary acidic protein (GFAP) antibody to detect astrocytes. Aβ plaque depositions were detected by 6E10. The primary antibodies are listed in Supplementary Table 1. High-magnification images were acquired using confocal laser scanning microscope (Olympus, FV3000). The area fraction of NeuN, MAP-2, CAA, Iba1, GFAP, 6E10-positive staining in cortex and hippocampus were quantified with ImageJ.

2.8. ELISA assays

The cortex and hippocampus were dissected rapidly on ice and sonicated in ice-cold lysis buffer. The lysate was centrifuged at 12,000×*g* for 10 min at 4 °C. The supernatant was collected to determine mouse interleukin-1β (IL-1β), interleukin-6 (IL-6), and tumor necrosis factor alpha (TNF-α) and interferon-γ (IFN-γ) in cortex and hippocampus were measured using corresponding ELISA kits (USCN, China).

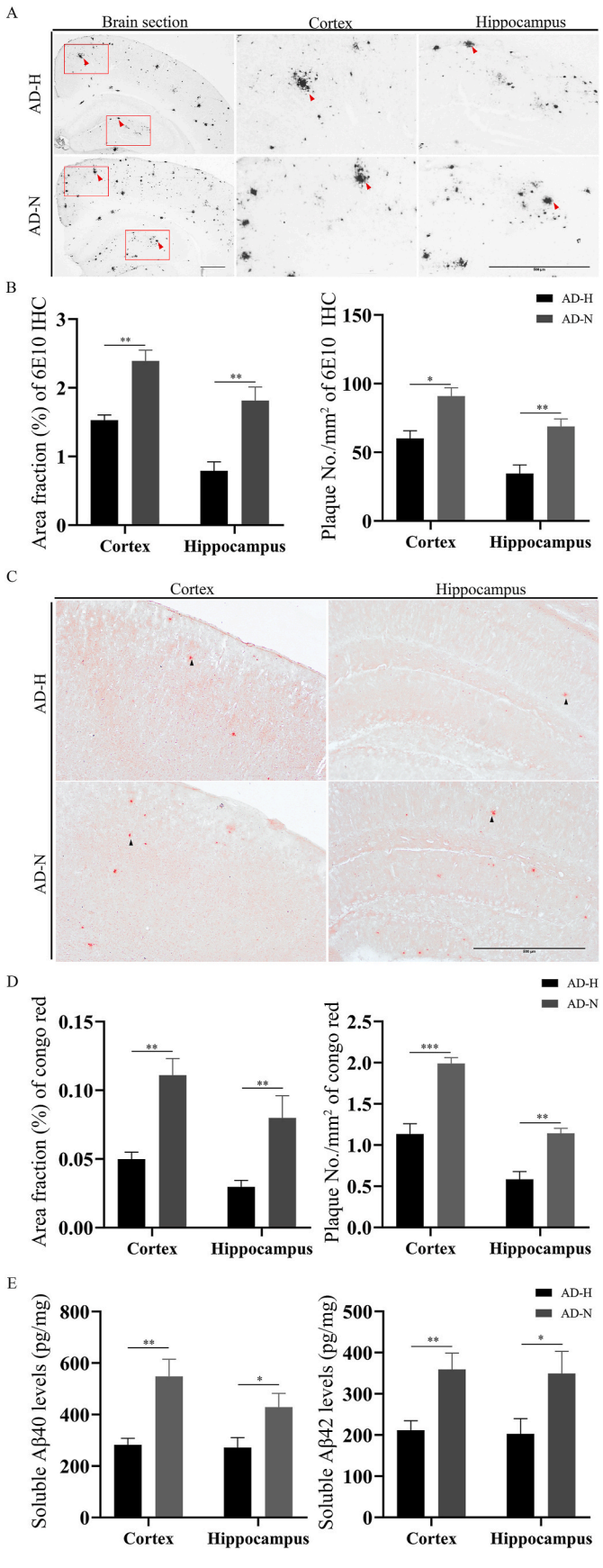

(caption on next column)

Fig. 2. HBOT alleviates Aβ pathology in the brain of AD mice. (A) Representative images 6E10 immunohistochemical staining in cortex and hippocampus in AD-H and AD-N mice. Scale bar = 500 μm. (B) Comparison of the area fraction and density of 6E10-positive Aβ plaques in the cortex and hippocampus between AD-H and AD-N mice. (C) Representative images of Congo red in cortex and hippocampus in AD-H and AD-N mice. (D) Comparison of the area fraction and density of Congo red in the cortex and hippocampus between AD-H and AD-N mice. (E) Comparison of Aβ40 and Aβ42 levels measured with ELISA of cortex and hippocampus between AD-H and AD-N mice. Data were the mean ± SEM values, with 6 mice per group.*$p < 0.05$, **$p < 0.01$, ***$p < 0.001$, ****$p < 0.0001$, by unpaired *t*-test. (For interpretation of the references to colour in this figure legend, the reader is referred to the Web version of this article.)

Homogenization was performed in an ice-cold tris/guanidine buffer (5 M guanidine hydrochloride/50 mM TrisCl, pH 8.0) using dissected cortex and hippocampus samples. Following the manufacturer's instructions, the levels of Aβ40 and Aβ42 were determined in samples using human-specific ELISA kits (Invitrogen, KHB3544, and KHB3481).

2.9. Western blotting

The western blotting protocol was described in our previous studies [26]. Briefly, hippocampal and cortex tissues were dissected and collected on ice, then sonicated and centrifuged. The supernatant was detected with protein concentration and used for further analysis. After SDS-PAGE gel running and transfer to the PVDF membrane, the membrane was blocked and incubated at 4 °C overnight with the primary antibodies listed in Supplementary Table 1. Then the membrane was incubated with secondary antibodies. The protein bands on the membrane were quantified with ImageJ.

2.10. Gene expression

Protocols for total RNA extraction, cDNA synthesis and quantitative real-time polymerase chain reaction (PCR) were described previously [11]. Cortex was dissected and extracted for total RNA with RNAiso Plus (Total RNA extraction reagent; Takara, Shiga, Japan). According to Revertra Ace qPCR RT kit (Takara, Shiga, Japan) instructions, total RNA was synthesized to cDNA. Real-time PCR was performed with TransStart Top Green qPCR SuperMix (TransGen Biotech, Beijing, China) and monitored by the Real-time PCR System (Bio-Rad CFX96 Real-Time PCR Systems). The primer sequences were provided upon request as summarized in Supplementary Table 2. The relative expression levels of each primer sequences mRNA were analyzed by the $2^{-\Delta\Delta}$Ct algorithm normalizing to GAPDH and relative to the control groups.

2.11. Statistical analysis

All data represent the mean ± SEM. Statistical analysis included 2-tailed Student's *t*-test for the comparison of two groups, and two-way ANOVA and Tukey's test for the comparison of multiple groups when required. Normality and equal-variance testing were performed for all assays. $P < 0.05$ was considered significant. Graphing and analysis were performed by GraphPad Prism 8 software.

3. Result

3.1. HBOT improves the performance of $APP^{swe}/PS1^{dE9}$ mice in behavioral tasks

During the 4-day training period Morris water maze, the incubation period of AD-H mice to find the platform on the 2nd day was shorter than that of AD-N mice ($p < 0.05$) (Fig. 1A). In the Morris water maze test period, the number of AD-H mice passing through the target position was increased compared with AD-N mice ($p < 0.05$); and AD-H mice

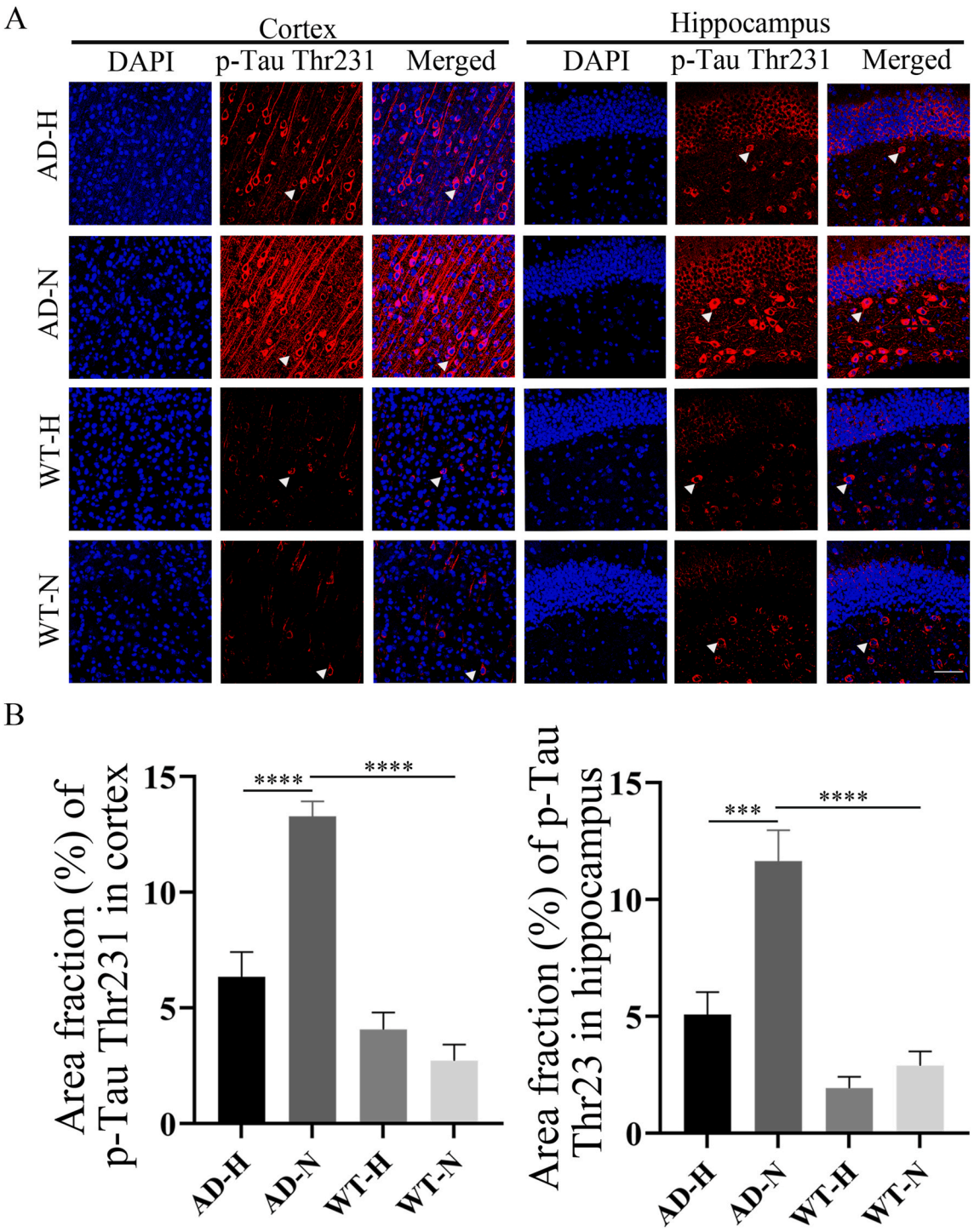

Fig. 3. Immunofluorescent staining of p-Tau Thr231 in the cortex and hippocampus of AD and WT mice after HBOT. (A) The level of p-Tau Thr231 positive neurons in the cortex and hippocampus of AD and WT mice after HBOT. scale bar = 100 μm. (B) Quantitative statistical analysis showed that fluorescence area of p-Tau Thr231 staining in the cortex and hippocampus of AD mice decreased after HBOT. Data were the mean ± SEM values, with 6 mice per group.*$p < 0.05$, **$p < 0.01$, ***$p < 0.001$, ****$p < 0.0001$, by two-way ANOVA with Tukey's multiple comparisons test.

spent more time in the target quadrant compared with AD-N mice ($p < 0.05$) (Fig. 1 B & C). In the shuttle box experiment, AD-H mice showed a higher frequency of active escape responses compared to AD-N mice ($p < 0.05$) (Fig. 1D). Besides, AD-H mice displayed significantly less passive escape responses compared to AD-N mice ($p < 0.05$) (Fig. 1E). In the open field test, AD-H mice exhibited an average of approximately 29 episodes of vertical exploration, which was more than that of around 14 episodes in AD-N mice ($p < 0.05$) (Fig. 1F). Moreover, AD-H mice demonstrated greater exploratory distances than the AD-N mice ($p < 0.05$) (Fig. 1G).

3.2. HBOT reduces brain amyloid deposition

To evaluate the effect of HBOT on Aβ deposition, we measured the SPs deposition profile in the cortex and hippocampus of $APP^{swe}/PS1^{dE9}$ mice. AD-H mice had a decreased level of Aβ plaques in the brain

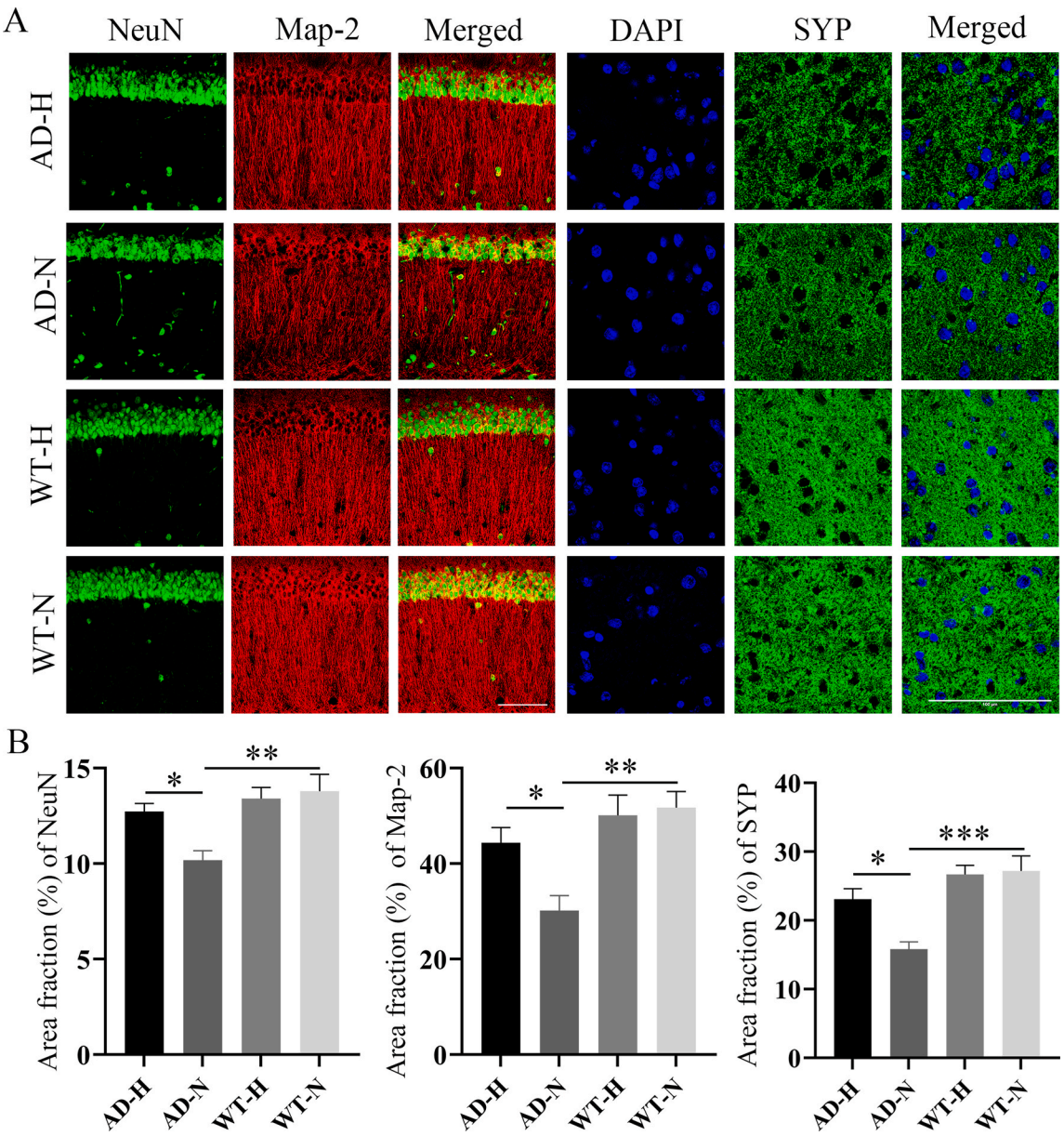

Fig. 4. NeuN + Map2 and SYP staining in the brain of AD and WT mice after HBOT. (A) The level of NeuN+Map2 and SYP in hippocampus of AD mice increased after HBOT. scale bar = 100 μm. (B) Quantitative statistical analysis showed that the fluorescence area of NeuN+map2 and SYP staining in the hippocampus of AD increased after HBOT. Data were the mean ± SEM values, with 6 mice per group. *$p < 0.05$, **$p < 0.01$, ***$p < 0.001$, ****$p < 0.0001$, by two-way ANOVA with Tukey's multiple comparisons test.

compared to AD-N mice, as shown by the 6E10 and Congo red positive plaque area percentage and the plaque number were lower than those in AD-N mice (Fig. 2A–D). And Aβ40 and Aβ42 levels measured with ELISA decreased in the cortex ($p < 0.01$) and hippocampus ($p < 0.05$) of AD mice after HBOT (Fig. 2E).

Further, the protein levels of β-site APP cleaving enzyme 1 (BACE1) were reduced in AD-H groups (Supplemental Fig.S1 A&B). There was no significant difference in Aβ-degrading enzyme (insulin degrading enzyme (IDE)), and Aβ transport receptors across BBB (low-density lipoprotein receptor-related protein-1(LRP-1)) in the brain between both groups (Supplemental Fig.S1 C-F).

3.3. Effect of HBOT on tau protein pathology

In order to determine the effect of HBOT on tau phosphorylation in cortex and hippocampus of $APP^{swe}/PS1^{dE9}$ and WT mice, we conducted immunofluorescence staining on p-tau Thr231 in the cortex and hippocampus of AD and WT mice (Fig. 3A&B). The area fractions of p-tau Thr231positive neurons in cortex and hippocampus of AD-H mice were lower than AD-N mice ($p < 0.05$) (Fig. 3A&B).

3.4. HBOT attenuates neuronal loss and synaptic degeneration

By co-staining of NeuN and Map2, the percentage of NeuN-positive area in hippocampus of AD-H mice was higher than that in AD-N mice ($p < 0.05$); and the percentage of MAP2-positive area was also higher than that of AD-N ($p < 0.05$) (Fig. 4 A&B). To verify the effect of HBOT on synaptic functions of $APP^{swe}/PS1^{dE9}$ and WT mice, we performed immunofluorescence staining on SYP (Fig. 4A&B). Quantitative statistical analysis found that the percentage of SYP positive area in the cortex of mice in AD-H was increased compared with that in AD-N ($p < 0.05$) (Fig. 4A&B).

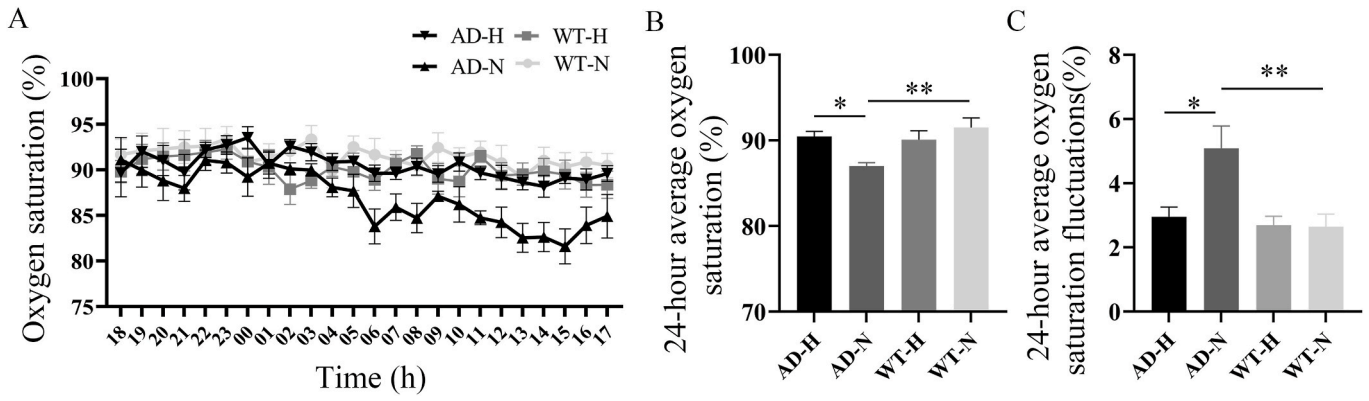

Fig. 5. HBOT improves blood oxygen saturation and ameliorates oxygen saturation fluctuations. (A) Changes of 24 h blood oxygen saturation in AD-H, AD-N, WT-H and WT-N mice. (B) The level of oxygen saturation of AD and WT mice after HBOT. (C) The level of oxygen saturation fluctuations of AD and WT mice after HBOT. Data were the mean ± SEM values, with 6 mice per group. *$p < 0.05$, **$p < 0.01$, ***$p < 0.001$, ****$p < 0.0001$, by two-way ANOVA with Tukey's multiple comparisons test.

3.5. HBOT improves blood oxygen saturation

Our study showed that HBOT continuously increased oxygen saturation level and ameliorated oxygen saturation fluctuations in AD mice for at least 3 months ($p < 0.05$) (Fig. 5 A – C). Further, our data also found that the red blood cell (RBC) count of $APP^{swe}/PS1^{dE9}$ mice increased after HBOT ($p < 0.05$) (Supplementary Table 3). Besides, HBOT also promoted the expression of HIF-1α in the brain of $APP^{swe}/PS1^{dE9}$ mice ($p < 0.05$) (Supplementary Fig. S2).

It is known that extreme high exposure level of oxygen may have the risk for oxidative damage to multiple organs and tissues such as lung, brain, blood vessels, etc. To investigate the potential oxidative damage caused by long-term HBOT, we assessed MDA levels in corresponding sites. The findings indicated that long-term HBOT did not elevate the MDA levels in lung tissue, brain tissue, and serum. Conversely, long-term HBOT was observed to reduce the MDA levels (Supplementary Fig. S3).

3.6. HBOT attenuates cerebrovascular hypoperfusion and microvascular injury

Impairments in cerebral circulation and vascular reactivity have substantial roles in onset and progression of AD. We investigated resting of CBF in both group at 9 months of age using laser speckle flowmetry. AD-H mice exhibited significantly increased CBF compared with AD-N mice ($p < 0.05$) (Fig. 6 A & B). With the antibody to 6E10 and smooth muscle in the vessel wall 1A4, compared with AD-N mice, AD-H mice had dramatic reductions Aβ deposition in vessel walls ($p < 0.05$) (Fig. 6C & D).

3.7. Effects of HBOT on the activation of microglia and astrocytes

In order to evaluate the effects of HBOT on glial cells in the brain of mice, immunofluorescence staining was performed on microglia and astrocytes in the cortex and hippocampus of four groups mice (Figs. 7 and 8). Iba1-positive microglia in the cortex and hippocampus of $APP^{swe}/PS1^{dE9}$ mice were reduced after HBOT treatment ($p < 0.05$) (Fig. 7). Meanwhile, AD-H mice displayed significantly fewer Aβ plaques in the brain compared to AD-N mice ($p < 0.05$) (Fig. 7). GFAP-positive astrocytes in the cortex and hippocampus of $APP^{swe}/PS1^{dE9}$ mice were reduced after HBOT treatment ($p < 0.05$) (Fig. 8). Meanwhile, ELISA detection method showed that after HBOT intervention, IL-1β, IL-6, TNF-α and IFN-γ inflammatory factors in the brain of AD and WT mice were reduced to a various degree compared with control mice ($p < 0.05$) (Fig. 9).

4. Discussion

In our studies, we firstly demonstrated that long-term HBOT attenuated the impairments in cognitive function observed in $APP^{swe}/PS1^{dE9}$ mice. Most importantly, HBOT effectively reduced the progression of amyloid plaque deposition, aggregation of hyperphosphorylated tau protein, and neuronal and synaptic degeneration in the AD mice.

Previous studies by our and other teams have demonstrated the potential of HBOT in ameliorating the pathological alterations seen in AD. However, these studies primarily focused on the short-term effects of HBOT on AD in the middle and late stages of the disease. AD is a continuous pathological process, there is a long period of asymptomatic stage before the onset of the disease. In this stage, the patients have not yet shown cognitive impairment, but amyloid deposition and neuronal fiber tangles have begun to appear [32]. With the development of the disease, AD tends to progress faster in the later stages. The asymptomatic phase of AD is the best time window to intervene this disease. Because the asymptomatic period is relatively longer than the symptomatic period, through the observation of several key pathophysiological changes of AD we may be able to identify the pharmacological or non-pharmacological therepies to delay, prevent, or even reverse the development of AD [33].

In addition, repeated exposure to HBOT over a long period of time is required to achieve lasting effects that cause changes in blood vessels, neurons, and cell activity [14,21]. Our study also proved for the first time that 90 consecutive days of HBOT still significantly improved AD-like cognitive function and pathological changes, which can provide a basis for subsequent clinical studies to develop HBOT treatment protocols for AD.

Meanwhile, the cognitive function and pathological changes of AD mice after a longer interval have not been reported. Therefore, this study examined the cognitive function and AD-like pathological changes of AD mice at 3 months after HBOT. Our study is the first to show that early and long-term HBOT of AD disease can effectively improve cognitive function and pathological impairment.

Oxygen is a rate-limiting factor in brain activity, and that HBOT directly increases oxygen levels and thus improves cognitive function [34]. In our previous study, blood oxygen saturation in $APP^{swe}/PS1^{dE9}$ mice was significantly lower than in WT mice [26]. In this experiment, we adopted male mice and found that $APP^{swe}/PS1^{dE9}$ mice not only had lower blood oxygen saturation, but also had higher fluctuation of blood oxygen saturation compared with WT mice. The oxygen saturation fluctuations analysis be used as a non-invasive measurement to determine the negative sequelae of hypoxemia [35]. And oxygen saturation fluctuations during graded hypoxia exposure carry information about cardio-respiratory control [36]. Increased fluctuation in oxygen

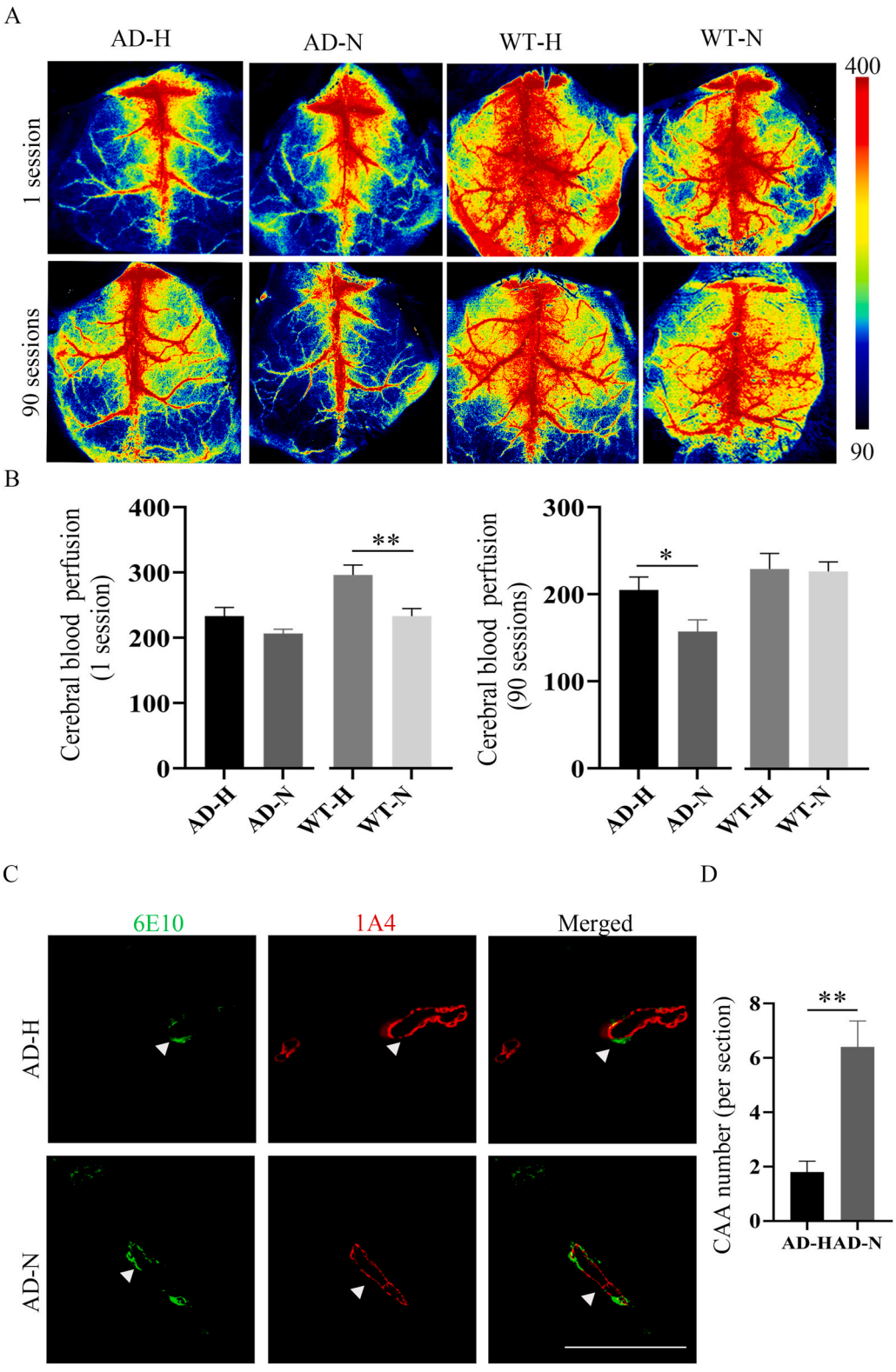

Fig. 6. HBOT attenuates cerebrovascular hypoperfusion and microvascular injury in the AD mice. (A) Cerebral perfusion images at age of 9 months in the control and HBOT groups (1 session and 90 sessions). (B) Histograms comparing the cerebral blood perfusion. (C) Representative images of 6E10+1A4 in AD-H and AD-N mice (scale bar = 100 μm). (D) Histograms comparing number of 6E10+1A4 in the AD-H and AD-N. Data were the mean ± SEM values, with 6 mice per group.*$p < 0.05$, **$p < 0.01$, ***$p < 0.001$, ****$p < 0.0001$, by unpaired *t*-test.

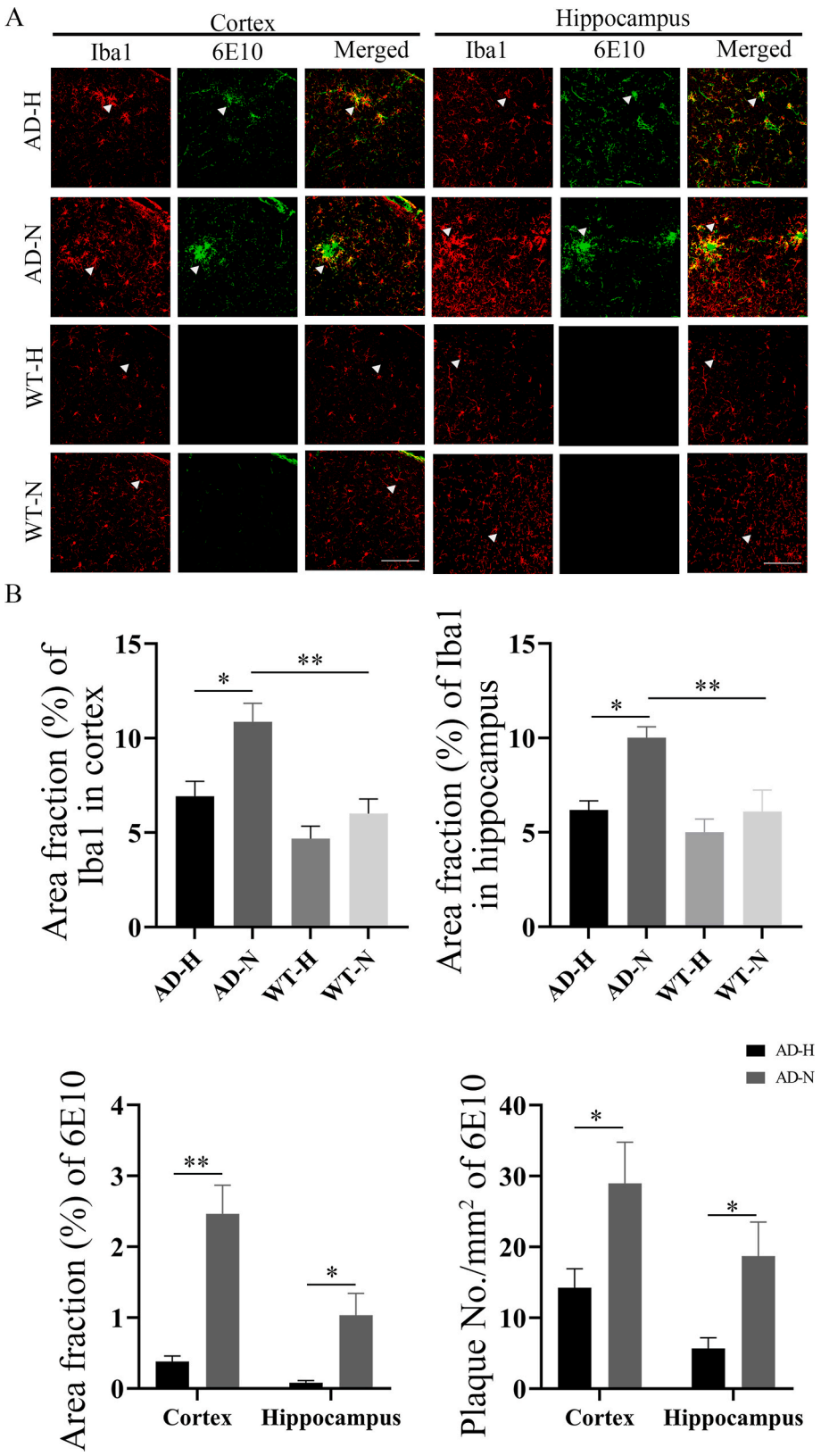

Fig. 7. Immunoflourescence staining of microglia cells in the cortex and hippocampus of AD and WT mice after HBOT. (A) Iba1 staining showed a reduced in microglia in the cortex and hippocampus of AD mice after HBOT, and 6E10 staining showed a significant decrease in Aβ plaques deposition in the cortex and hippocampus of AD mice after HBOT (scale bar = 100 μm). (B) Statistical analysis showed that the staining positive area of microglia in the cortex and hippocampus of AD mice after HBOT was decreased, and the Aβ plaques area fraction and density in the cortex and hippocampus of AD mice after HBOT was decreased. Data were the mean ± SEM values, with 6 mice per group.*$p < 0.05$, **$p < 0.01$, ***$p < 0.001$, ****$p < 0.0001$, by unpaired *t*-test and two-way ANOVA with Tukey's multiple comparisons test.

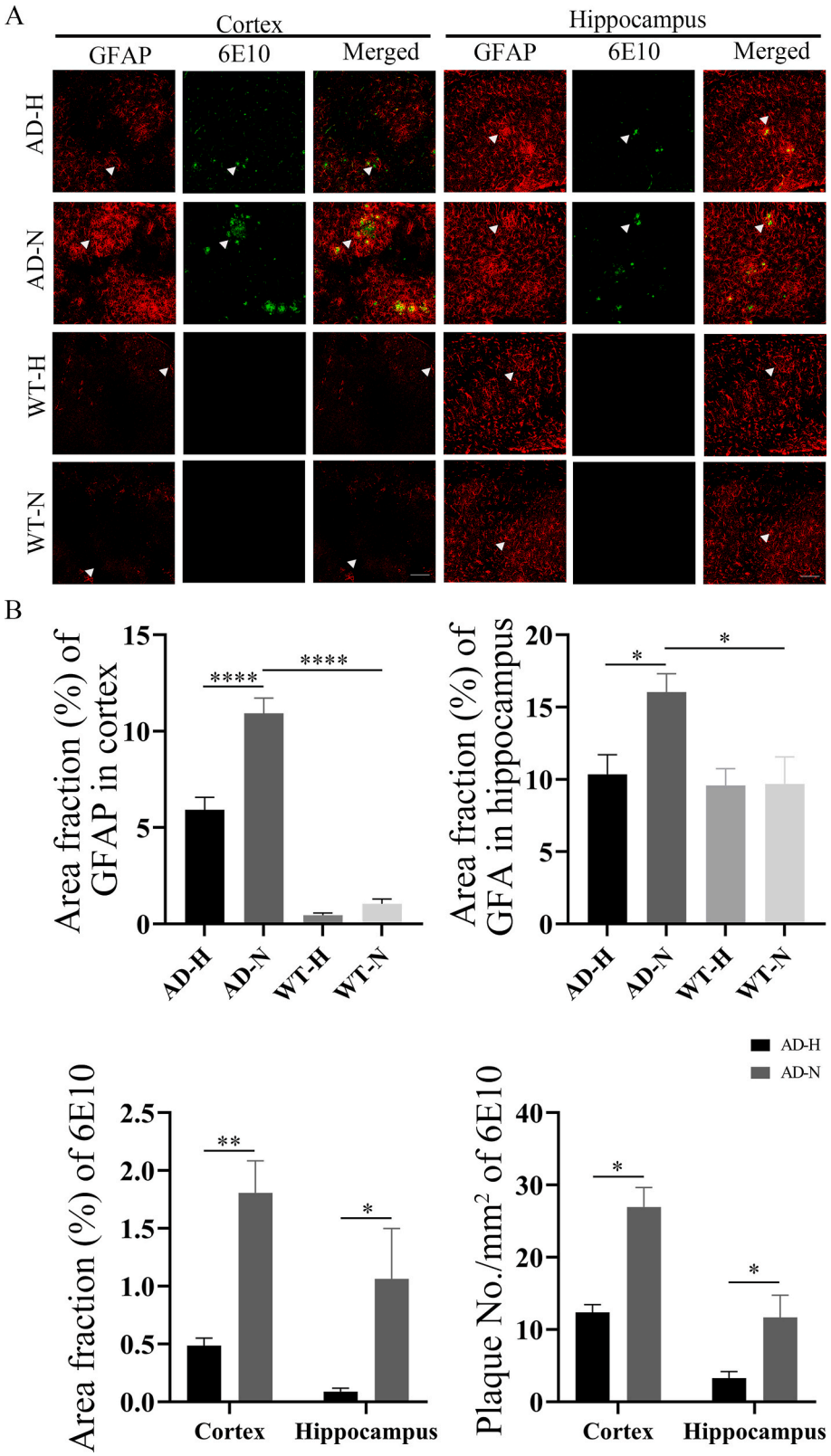

Fig. 8. Immunoflourescence staining of astrocytes in the cortex and hippocampus of AD and WT mice after HBOT. (A) GFAP staining showed a reduced in astrocytes in the cortex and hippocampus of AD mice after HBOT, and 6E10 staining showed a decrease in Aβ plaques deposition in the cortex and hippocampus of AD mice after HBOT (scale bar = 100 μm). (B) Statistical analysis showed that the staining positive area of astrocytes in the cortex and hippocampus of AD mice after HBOT was significantly decreased, and the Aβ plaques area fraction and density in the cortex of AD mice after HBOT was significantly decreased. Data were the mean ± SEM values, with 6 mice per group.*$p < 0.05$, **$p < 0.01$, ***$p < 0.001$, ****$p < 0.0001$, by unpaired *t*-test and two-way ANOVA with Tukey's multiple comparisons test.

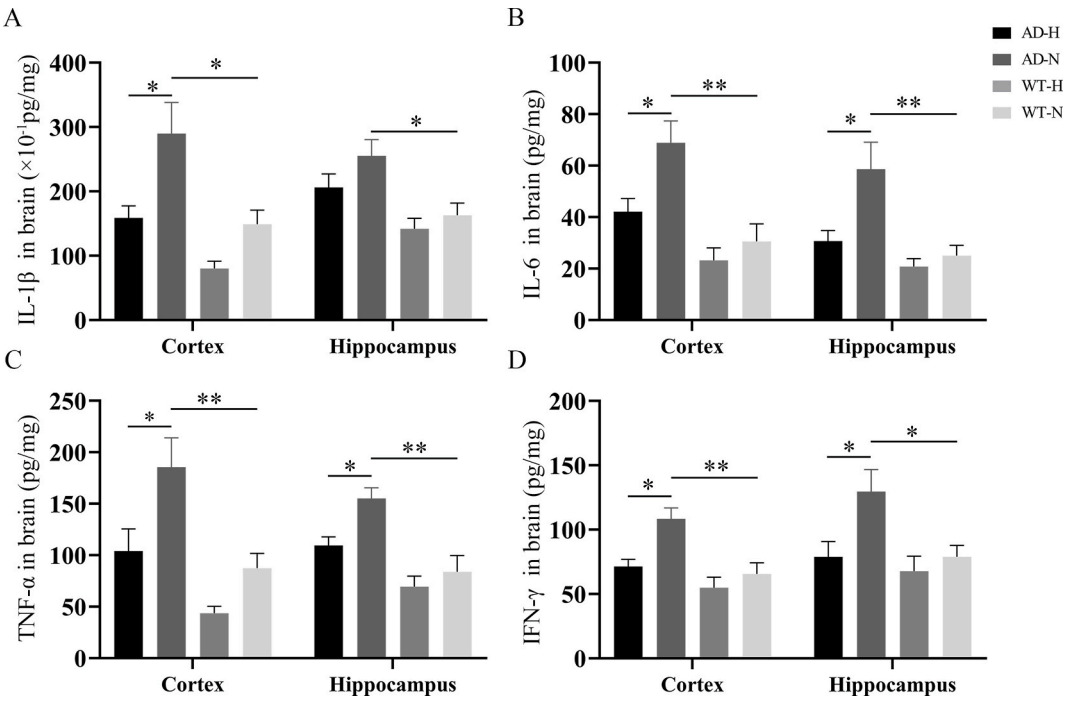

Fig. 9. Levels of inflammatory cytokines in the cortex and hippocampus of AD and WT mice after HBOT. (A)–(D) The expressions of pro-inflammatory cytokines IL-1β, IL-6, TNF-α and IFN-γ in the cortex and hippocampus of AD mice were decreased after HBOT treatment. Data were the mean ± SEM values, with 6 mice per group.*$p < 0.05$, **$p < 0.01$, ***$p < 0.001$, ****$p < 0.0001$, by two-way ANOVA with Tukey's multiple comparisons test.

saturation suggests an adverse prognosis [37]. Our study firstly showed that HBOT significantly improves the oxygen saturation and oxygen reserve of the body.

Oxidative stress is believed to play an important role in the pathogenesis of several neurodegenerative disorders [38]. Notably, high level of oxygen exposure can result in oxidative damage to lung tissue, brain tissue, and the entire body. MDA serves as an indicator for evaluating the degree of oxidative damage in tissues, cells, and cell membrane lipid peroxidation. To investigate the potential oxidative damage caused by long-term HBOT, we assessed the MDA levels in lung tissue, brain tissue, and serum. The findings indicated that long-term HBOT did not elevate the MDA levels in lung tissue, brain tissue, and serum. Conversely, long-term HBOT was observed to reduce the MDA levels to some extent (Supplementary Fig. S3.). This suggests that long-term HBOT does not cause peroxidation damage to the lung and blood system.

Further, our data showed that the RBC count of $APP^{swe}/PS1^{dE9}$ mice increased after long-term HBOT. Our and other groups have found a reduced number of RBC in $APP^{swe}/PS1^{dE9}$ [26,39]. And the short-term effect of hyperbaric oxygen on RBCs is to decrease the number of red blood cells, but the long-term effect of hyperbaric oxygen is to increase the number of RBCs [40]. This may be because repeated exposure to HBOT over a long period of time may activate HIF-1α which is involved in erythropoiesis, angiogenesis, and vascular remodeling [41]. This is based on the fact that oxygen level increase from 21 % to 100 % during HBOT treatment and decrease again to 21 % at the end of each treatment. The reduction of oxygen content from 100 % to 21 % can be interpreted as a signal of hypoxia and activation of HIF-1α [21]. According to our team's previous research [42], HIF-1α protein levels were down-regulated in AD mice. In our study, long-term HBOT also promoted the expression of HIF-1α in the brain of $APP^{swe}/PS1^{dE9}$ mice (Supplementary Fig. S2.). Therefore, in this study, long-term HBOT promoted the production and number of red blood cells in the body.

Besides, long-term HBOT also improves vascular structure and dysfunction in $APP^{swe}/PS1^{dE9}$ mice. Reduced CBF in AD can be induced by numerous factors including cerebral amyloid angiopathy [43]. CAA is one of the major causes of vascular dysfunction in AD, as plaque accumulation impinges on blood vessels restricting cerebral blood flow [43]. In AD, significant changes occur in the cellular, morphological, and structural aspects of the cerebral vasculature, leading to alterations in blood flow regulation, vascular fluid dynamics, and vessel integrity [44]. HBOT triggers a broad range of vascular molecular mechanisms that encompass vascular structure, molecular adhesion and transport, and vascular signal transduction. These mechanisms effectively enhance the structure and function of blood vessels [22,45]. A grown of evidence from both AD and other forms of cognitive impairment suggests that decreases in blood flow may hinder Aβ clearance from the brain because of hypoxia, which may further facilitate Aβ production and inflammation. Thus, reductions hypoxia via HBOT would inhibit the pathologic feedback loop of blood flow reduction mediated hypoxia, Aβ accumulation and the progression of AD.

Repeated exposure to HBOT over a long period of time, in addition to the sustained effects of changes in neurons, red blood cells, and blood vessels, can also cause lasting changes in glial cells [21]. AD and neuroinflammation are closely related and form a vicious cycle in which one increases the pathological burden of the other [46,47]. Neuroinflammatory glial overreaction and protein accumulation are two prominent features of the aged brain and hallmarks of AD [48]. Another important effect of HBOT in several brain dysfunctions is the neuroinflammation reduction. In a TBI rat model, HBOT was shown to reduce neuroinflammation and increase levels of the IL-10; these changes were associated with improvements in cognitive deficit [49]. HBOT reversed hypoxia and ameliorated brain pathology, and improved the animals' behavioral performance [50]. This improvement was also associated with a reduction in proinflammatory cytokines such as IL-1β, IL-6, TNF-α. HBOT also significantly improved recovery from sepsis following cecal ligation and puncture [21]. The treatment was associated with a reduction in the inflammatory response, including decreased expression of TNF-α, IL-6, and IL-10 [21]. Consistent with those studies, our results show that long-term HBOT significantly attenuates the activation of microglia and astrocytes, decreases the levels of TNF-α, IL-6, and IL-1β.

Based on our findings, it is the first to demonstrate that long-term

HBOT intervention during the early stages of AD can improve AD-like pathological changes by enhancing the function and structure of neurons, glia, and blood vessels. Importantly, the therapeutic effects of long-term HBOT on AD are sustained even after the intervention is discontinued, suggesting that the benefits of long-term HBOT are not invalidated by the interruption of treatment. These results highlight the potential of long-term HBOT as a promising therapeutic approach for AD, particularly when administered early in the disease progression.

Indeed, future clinical trial of HBOT therapy is critical to test its safety and efficacy for the prevention and treatment of AD. Simultaneously, basic research efforts will continue to expand our understanding of the underlying mechanisms by which HBOT exerts its therapeutic effects in AD. By delving deeper into these mechanisms, researchers can identify specific pathways and processes that are involved in the positive outcomes of HBOT. This information is essential in optimizing treatment conditions, including determining the ideal duration, frequency, and overall treatment regimen for HBOT in AD. It is worth noting that the effects of HBOT on AD are likely not mediated by a single pathway but rather involve multiple interconnected mechanisms. Therefore, a comprehensive understanding of these mechanisms is essential for developing targeted and effective HBOT interventions for AD. Continued collaboration between clinical trials and basic research will pave the way for advancements in HBOT as a potential therapeutic approach for AD.

Authors' contributions

The research study was conceived and conceptualized by: Weidong Le. Research was designed by Weidong Le and Cui Yang. Experiments were performed and analyzed by Cui Yang and Gaungdong Liu. Manuscript draft was written by Cui Yang, edited by Weidong le, Xi Chen, Yang Xiang. Funding was provided by Weidong Le and Xi Chen. Resources were given by Weidong Le and Xianrong Zeng. All authors have read and approved the final manuscript.

Declaration of competing interest

Authors declare that there are no conflicts of interest.

Data availability

Data will be made available on request.

Acknowledgments

This work was supported by funding from the National Natural Science Foundation of China (32220103006 and 82271524), the Science and Technology project of Sichuan Province (2022ZDZX0023), and the Key Research and Development Program of Sichuan (2021YFS0382).

Appendix A. Supplementary data

Supplementary data to this article can be found online at https://doi.org/10.1016/j.redox.2023.103006.

References

[1] C. Reitz, C. Brayne, R. Mayeux, Epidemiology of alzheimer disease, Nat. Rev. Neurol. 7 (3) (2011) 137–152, https://doi.org/10.1038/nrneurol.2011.2.
[2] M.Y. Tang, F.A. Gorin, P.J. Lein, Review of evidence implicating the plasminogen activator system in blood-brain barrier dysfunction associated with Alzheimer's disease, Ageing Neurodegener Dis 2 (2022), https://doi.org/10.20517/and.2022.05.
[3] H. Liu, H. Qiu, J. Yang, J. Ni, W. Le, Chronic hypoxia facilitates Alzheimer's disease through demethylation of gamma-secretase by downregulating DNA methyltransferase 3b, Alzheimers Dement 12 (2) (2016) 130–143, https://doi.org/10.1016/j.jalz.2015.05.019.
[4] J. Cummings, Anti-amyloid monoclonal antibodies are transformative treatments that redefine alzheimer's disease therapeutics, Drugs 83 (7) (2023) 569–576, https://doi.org/10.1007/s40265-023-01858-9.
[5] E. Jutkowitz, L.T. Pizzi, P. Shewmaker, F. Alarid-Escudero, G. Epstein-Lubow, K. M. Prioli, J.E. Gaugler, L.N. Gitlin, Cost effectiveness of non-drug interventions that reduce nursing home admissions for people living with dementia, Alzheimers Dement 19 (9) (2023) 3867–3893, https://doi.org/10.1002/alz.12964.
[6] M. Su, D. Nizamutdinov, H. Liu, J.H. Huang, Recent mechanisms of neurodegeneration and photobiomodulation in the context of alzheimer's disease, Int. J. Mol. Sci. 24 (11) (2023), https://doi.org/10.3390/ijms24119272.
[7] T.H. Lin, Y.C. Liao, K.W. Tam, L. Chan, T.H. Hsu, Effects of music therapy on cognition, quality of life, and neuropsychiatric symptoms of patients with dementia: a systematic review and meta-analysis of randomized controlled trials, Psychiatr. Res. 329 (2023) 115498, https://doi.org/10.1016/j.psychres.2023.115498.
[8] P.L. Valenzuela, A. Castillo-Garcia, J.S. Morales, P. de la Villa, H. Hampel, E. Emanuele, S. Lista, A. Lucia, Exercise benefits on Alzheimer's disease: state-of-the-science, Ageing Res. Rev. 62 (2020) 101108, https://doi.org/10.1016/j.arr.2020.101108.
[9] C. Reitz, R. Mayeux, Alzheimer disease: epidemiology, diagnostic criteria, risk factors and biomarkers, Biochem. Pharmacol. 88 (4) (2014) 640–651, https://doi.org/10.1016/j.bcp.2013.12.024.
[10] H. Liu, H. Qiu, Q. Xiao, W. Le, Chronic hypoxia-induced autophagy aggravates the neuropathology of alzheimer's disease through AMPK-mTOR signaling in the APPSwe/PS1dE9 mouse model, J Alzheimers Dis 48 (4) (2015) 1019–1032, https://doi.org/10.3233/JAD-150303.
[11] F. Zhang, R. Zhong, H. Qi, S. Li, C. Cheng, X. Liu, Y. Liu, W. Le, Impacts of acute hypoxia on alzheimer's disease-like pathologies in APP(swe)/PS1(dE9) mice and their wild type littermates, Front. Neurosci. 12 (2018) 314, https://doi.org/10.3389/fnins.2018.00314.
[12] F. Zhang, L. Niu, S. Li, W. Le, Pathological impacts of chronic hypoxia on alzheimer's disease, ACS Chem. Neurosci. 10 (2) (2019) 902–909, https://doi.org/10.1021/acschemneuro.8b00442.
[13] Q. Fu, R. Duan, Y. Sun, Q. Li, Hyperbaric oxygen therapy for healthy aging: from mechanisms to therapeutics, Redox Biol. 53 (2022) 102352, https://doi.org/10.1016/j.redox.2022.102352.
[14] N. Schottlender, I. Gottfried, U. Ashery, Hyperbaric oxygen treatment: effects on mitochondrial function and oxidative stress, Biomolecules 11 (12) (2021), https://doi.org/10.3390/biom11121827.
[15] K. Thiankhaw, N. Chattipakorn, S.C. Chattipakorn, The effects of hyperbaric oxygen therapy on the brain with middle cerebral artery occlusion, J. Cell. Physiol. 236 (3) (2021) 1677–1694, https://doi.org/10.1002/jcp.29955.
[16] X.A. Figueroa, J.K. Wright, Hyperbaric oxygen: B-level evidence in mild traumatic brain injury clinical trials, Neurology 87 (13) (2016) 1400–1406, https://doi.org/10.1212/WNL.0000000000003146.
[17] G. Liu, C. Yang, X. Wang, X. Chen, Y. Wang, W. Le, Oxygen metabolism abnormality and Alzheimer's disease: an update, Redox Biol. 68 (2023) 102955, https://doi.org/10.1016/j.redox.2023.102955.
[18] V. Calabrese, J. Giordano, A. Signorile, M. Laura Ontario, S. Castorina, C. De Pasquale, G. Eckert, E.J. Calabrese, Major pathogenic mechanisms in vascular dementia: roles of cellular stress response and hormesis in neuroprotection, J. Neurosci. Res. 94 (12) (2016) 1588–1603, https://doi.org/10.1002/jnr.23925.
[19] H. Zhang, Y. Wang, D. Lyu, Y. Li, W. Li, Q. Wang, Y. Li, Q. Qin, X. Wang, M. Gong, H. Jiao, W. Liu, J. Jia, Cerebral blood flow in mild cognitive impairment and Alzheimer's disease: a systematic review and meta-analysis, Ageing Res. Rev. 71 (2021) 101450, https://doi.org/10.1016/j.arr.2021.101450.
[20] R.B. Nielsen, L. Egefjord, H. Angleys, K. Mouridsen, M. Gejl, A. Moller, B. Brock, H. Braendgaard, H. Gottrup, J. Rungby, S.F. Eskildsen, L. Ostergaard, Capillary dysfunction is associated with symptom severity and neurodegeneration in Alzheimer's disease, Alzheimers Dement 13 (10) (2017) 1143–1153, https://doi.org/10.1016/j.jalz.2017.02.007.
[21] I. Gottfried, N. Schottlender, U. Ashery, Hyperbaric oxygen treatment-from mechanisms to cognitive improvement, Biomolecules 11 (10) (2021), https://doi.org/10.3390/biom11101520.
[22] A. Hadanny, M. Daniel-Kotovsky, G. Suzin, R. Boussi-Gross, M. Catalogna, K. Dagan, Y. Hachmo, R. Abu Hamed, E. Sasson, G. Fishlev, E. Lang, N. Polak, K. Doenyas, M. Friedman, S. Tal, Y. Zemel, Y. Bechor, S. Efrati, Cognitive enhancement of healthy older adults using hyperbaric oxygen: a randomized controlled trial, Aging (Albany NY) 12 (13) (2020) 13740–13761, https://doi.org/10.18632/aging.103571.
[23] F. Leng, P. Edison, Neuroinflammation and microglial activation in Alzheimer disease: where do we go from here? Nat. Rev. Neurol. 17 (3) (2021) 157–172, https://doi.org/10.1038/s41582-020-00435-y.
[24] T. Shwe, C. Bo-Htay, B. Ongnok, T. Chunchai, T. Jaiwongkam, S. Kerdphoo, S. Kumfu, W. Pratchayasakul, T. Pattarasakulchai, N. Chattipakorn, S. C. Chattipakorn, Hyperbaric oxygen therapy restores cognitive function and hippocampal pathologies in both aging and aging-obese rats, Mech. Ageing Dev. 195 (2021) 111465, https://doi.org/10.1016/j.mad.2021.111465.
[25] I. Lavrnja, A. Parabucki, P. Brkic, T. Jovanovic, S. Dacic, D. Savic, I. Pantic, M. Stojiljkovic, S. Pekovic, Repetitive hyperbaric oxygenation attenuates reactive astrogliosis and suppresses expression of inflammatory mediators in the rat model of brain injury, Mediat. Inflamm. 2015 (2015) 498405, https://doi.org/10.1155/2015/498405.
[26] M. Wang, X. Chen, L. Niu, J. Xu, H. Yu, X. Xu, Q. Yang, Y. Xiang, W. Le, APP(swe)/PS1(DeltaE9) mice exhibit low oxygen saturation and alterations of erythrocytes

preceding the neuropathology and cognitive deficiency during Alzheimer's disease, CNS Neurosci. Ther. (2023), https://doi.org/10.1111/cns.14147.
[27] H.R. Weiss, J. Grayson, X. Liu, S. Barsoum, H. Shah, O.Z. Chi, Cerebral ischemia and reperfusion increases the heterogeneity of local oxygen supply/consumption balance, Stroke 44 (9) (2013) 2553–2558, https://doi.org/10.1161/STROKEAHA.113.001172.
[28] K. Cao, J. Xiang, Y.T. Dong, Y. Xu, Y. Li, H. Song, X.X. Zeng, L.Y. Ran, W. Hong, Z. Z. Guan, Exposure to fluoride aggravates the impairment in learning and memory and neuropathological lesions in mice carrying the APP/PS1 double-transgenic mutation, Alzheimer's Res. Ther. 11 (1) (2019) 35, https://doi.org/10.1186/s13195-019-0490-3.
[29] S. Saito, Y. Yamamoto, T. Maki, Y. Hattori, H. Ito, K. Mizuno, M. Harada-Shiba, R. N. Kalaria, M. Fukushima, R. Takahashi, M. Ihara, Taxifolin inhibits amyloid-beta oligomer formation and fully restores vascular integrity and memory in cerebral amyloid angiopathy, Acta Neuropathol Commun 5 (1) (2017) 26, https://doi.org/10.1186/s40478-017-0429-5.
[30] C. Ye, Y. Liang, Y. Chen, Y. Xiong, Y. She, X. Zhong, H. Chen, M. Huang, Berberine improves cognitive impairment by simultaneously impacting cerebral blood flow and beta-amyloid accumulation in an APP/tau/PS1 mouse model of alzheimer's disease, Cells 10 (5) (2021), https://doi.org/10.3390/cells10051161.
[31] S. Tarantini, A. Nyul-Toth, A. Yabluchanskiy, T. Csipo, P. Mukli, P. Balasubramanian, A. Ungvari, P. Toth, Z. Benyo, W.E. Sonntag, Z. Ungvari, A. Csiszar, Endothelial deficiency of insulin-like growth factor-1 receptor (IGF1R) impairs neurovascular coupling responses in mice, mimicking aspects of the brain aging phenotype, Geroscience 43 (5) (2021) 2387–2394, https://doi.org/10.1007/s11357-021-00405-2.
[32] W.K. Self, D.M. Holtzman, Emerging diagnostics and therapeutics for Alzheimer disease, Nat. Med. (2023), https://doi.org/10.1038/s41591-023-02505-2.
[33] W. Liu, S. Gauthier, J. Jia, Alzheimer's disease: current status and perspective, Sci. Bull. 67 (24) (2022) 2494–2497, https://doi.org/10.1016/j.scib.2022.12.006.
[34] D. Vadas, L. Kalichman, A. Hadanny, S. Efrati, Hyperbaric oxygen environment can enhance brain activity and multitasking performance, Front. Integr. Neurosci. 11 (2017) 25, https://doi.org/10.3389/fnint.2017.00025.
[35] J.T. Costello, A.S. Bhogal, T.B. Williams, R. Bekoe, A. Sabir, M.J. Tipton, J. Corbett, A.R. Mani, Effects of normobaric hypoxia on oxygen saturation variability, High Alt. Med. Biol. 21 (1) (2020) 76–83, https://doi.org/10.1089/ham.2019.0092.
[36] Y. Jiang, J.T. Costello, T.B. Williams, N. Panyapiean, A.S. Bhogal, M.J. Tipton, J. Corbett, A.R. Mani, A network physiology approach to oxygen saturation variability during normobaric hypoxia, Exp. Physiol. 106 (1) (2021) 151–159, https://doi.org/10.1113/EP088755.
[37] H. Zhang, I. Campos, L. Chan, A. Meyring-Wosten, L.M. Tapia Silva, L. Rivera Fuentes, P. Preciado, S. Thijssen, J.P. Kooman, F.M. van der Sande, P. Kotanko, Association of central venous oxygen saturation variability and mortality in hemodialysis patients, Blood Purif. 47 (1–3) (2019) 246–253, https://doi.org/10.1159/000494630.
[38] V. Calabrese, C. Mancuso, A. Ravagna, M. Perluigi, C. Cini, C. De Marco, D. A. Butterfield, A.M. Stella, In vivo induction of heat shock proteins in the substantia nigra following L-DOPA administration is associated with increased activity of mitochondrial complex I and nitrosative stress in rats: regulation by glutathione redox state, J. Neurochem. 101 (3) (2007) 709–717, https://doi.org/10.1111/j.1471-4159.2006.04367.x.
[39] A. Stevenson, D. Lopez, P. Khoo, R.N. Kalaria, E.B. Mukaetova-Ladinska, Exploring erythrocytes as blood biomarkers for alzheimer's disease, J Alzheimers Dis 60 (3) (2017) 845–857, https://doi.org/10.3233/JAD-170363.
[40] A.E. Gunes, S. Aktas, Effect of hyperbaric oxygen therapy on complete blood count, Undersea Hyperb. Med. 44 (4) (2017) 357–364, https://doi.org/10.22462/7.8.2017.8.
[41] T. Ollonen, M. Kurkela, A. Laitakari, S. Sakko, H. Koivisto, J. Myllyharju, H. Tanila, R. Serpi, P. Koivunen, Activation of the hypoxia response protects mice from amyloid-beta accumulation, Cell. Mol. Life Sci. 79 (8) (2022) 432, https://doi.org/10.1007/s00018-022-04460-6.
[42] X. Zhang, L. Li, X. Zhang, W. Xie, L. Li, D. Yang, X. Heng, Y. Du, R.S. Doody, W. Le, Prenatal hypoxia may aggravate the cognitive impairment and Alzheimer's disease neuropathology in APPSwe/PS1A246E transgenic mice, Neurobiol. Aging 34 (3) (2013) 663–678, https://doi.org/10.1016/j.neurobiolaging.2012.06.012.
[43] E. Park, L.Y. Li, C. He, A.Z. Abbasi, T. Ahmed, W.D. Foltz, R. O'Flaherty, M. Zain, R. P. Bonin, A.M. Rauth, P.E. Fraser, J.T. Henderson, X.Y. Wu, Brain-penetrating and disease site-targeting manganese dioxide-polymer-lipid hybrid nanoparticles remodel microenvironment of alzheimer's disease by regulating multiple pathological pathways, Adv. Sci. 10 (12) (2023) e2207238, https://doi.org/10.1002/advs.202207238.
[44] J. Klohs, An integrated view on vascular dysfunction in alzheimer's disease, Neurodegener. Dis. 19 (3–4) (2019) 109–127, https://doi.org/10.1159/000505625.
[45] R. Shapira, A. Gdalyahu, I. Gottfried, E. Sasson, A. Hadanny, S. Efrati, P. Blinder, U. Ashery, Hyperbaric oxygen therapy alleviates vascular dysfunction and amyloid burden in an Alzheimer's disease mouse model and in elderly patients, Aging (Albany NY) 13 (17) (2021) 20935–20961, https://doi.org/10.18632/aging.203485.
[46] H. Hampel, F. Caraci, A.C. Cuello, G. Caruso, R. Nistico, M. Corbo, F. Baldacci, N. Toschi, F. Garaci, P.A. Chiesa, S.R. Verdooner, L. Akman-Anderson, F. Hernandez, J. Avila, E. Emanuele, P.L. Valenzuela, A. Lucia, M. Watling, B. P. Imbimbo, A. Vergallo, S. Lista, A path toward precision medicine for neuroinflammatory mechanisms in alzheimer's disease, Front. Immunol. 11 (2020) 456, https://doi.org/10.3389/fimmu.2020.00456.
[47] V. Calabrese, C. Cornelius, A.T. Dinkova-Kostova, E.J. Calabrese, M.P. Mattson, Cellular stress responses, the hormesis paradigm, and vitagenes: novel targets for therapeutic intervention in neurodegenerative disorders, Antioxidants Redox Signal. 13 (11) (2010) 1763–1811, https://doi.org/10.1089/ars.2009.3074.
[48] V. Astillero-Lopez, M. Gonzalez-Rodriguez, S. Villar-Conde, A. Flores-Cuadrado, A. Martinez-Marcos, I. Ubeda-Banon, D. Saiz-Sanchez, Neurodegeneration and astrogliosis in the entorhinal cortex in Alzheimer's disease: stereological layer-specific assessment and proteomic analysis, Alzheimers Dement 18 (12) (2022) 2468–2480, https://doi.org/10.1002/alz.12580.
[49] K.C. Lin, K.C. Niu, K.J. Tsai, J.R. Kuo, L.C. Wang, C.C. Chio, C.P. Chang, Attenuating inflammation but stimulating both angiogenesis and neurogenesis using hyperbaric oxygen in rats with traumatic brain injury, J. Trauma Acute Care Surg. 72 (3) (2012) 650–659, https://doi.org/10.1097/TA.0b013e31823c575f.
[50] R. Shapira, B. Solomon, S. Efrati, D. Frenkel, U. Ashery, Hyperbaric oxygen therapy ameliorates pathophysiology of 3xTg-AD mouse model by attenuating neuroinflammation, Neurobiol. Aging 62 (2018) 105–119, https://doi.org/10.1016/j.neurobiolaging.2017.10.007.